Transactions of the 17th International Conference on Structural Mechanics in Reactor Technology (SMiRT 17)
Prague, Czech Republic, August 17 –22, 2003
Paper # F02-5

Industrial Models for Thermal Fatigue Crack Initiation and Propagation in Mixing Zones of Piping Systems

Frédéric Beaud[1)], Stéphanie Musi[1)], Claude Faidy[1)]

[1)] EDF, Energy Branch, Basic Design Department

ABSTRACT

Piping systems of nuclear power plants include connections of branches conveying fluids at different temperatures. Thermal-hydraulic fluctuations arising from the turbulent mixing of the flows can possibly affect the inner wall of the pipes and lead to fatigue damage. This paper aims at describing the different steps of the selection and analysis of the sensitive mixing zones.

KEY WORDS : mixing, fluctuations, temperature, stress, damage, thermal striping, crack, initiation, propagation, nuclear, power plant, fatigue, growth, stress intensity factor, methodology

INTRODUCTION

Piping systems of nuclear power plants include connections of branches conveying fluids at different temperatures. Thermal-hydraulic fluctuations arise from the turbulent mixing of the flows and result in temperature and stress fluctuations through the wall of the pipe. In addition to the normal operating transients, they contribute to fatigue damage of the structure and can lead to thermal striping and through-wall cracks. Civaux 1 plant was shut down in May 1998 following a leak of primary coolant from a pipe elbow in the residual heat removal (RHR) system [1]. Afterwards, other RHR mixing zones turned out to be concerned by this fatigue phenomenon.

As this kind of phenomenon was not taken into account at the design stage, no appropriate methodology was available, first to explain RHR damages, then to justify replacement parts and in-service inspections, and finally to analyze mixing zones in other systems. Industrial methodologies for both crack initiation and propagation analyses based upon simplified thermal and mechanical hypotheses have thus been developed. The procedure includes the following successive steps [1] :

1. Crack initiation evaluation
   - Use of a screening criteria based upon a threshold value of the upstream temperature difference ΔT ;
   - Taking into account the duration by developing a set of curves (ΔT, number of hours), based on a consistent approach.
2. Detailed mechanical analysis of crack propagation (among complementary studies including repair, monitor, operating conditions, modifications… which are not addressed here).

In a first part, the screening criteria for the selection of sensitive mixing zones are presented and the analytical solution of the thermal-mechanical problem is derived. In a second part, the detailed analysis of sensitive mixing zones is explained. The last part presents possible improvements of the methodologies and on-going R&D programs at EDF.

SCREENING CRITERIA FOR THE SELECTION OF SENSITIVE MIXING ZONES

First Step : ΔT Threshold Value

The first step of the procedure used by EDF consists in the comparison between the maximal value of the temperature difference upstream the mixing zone and a threshold value depending on the material (80°C for stainless steel and 50°C for carbon and low alloy steel).

Mixing zones always operating below this threshold value are not subjected to fatigue crack initiation.

Second Step : $\Delta T=f(t)$ Curves

From the operating conditions (ΔT and corresponding operating time t), this step allows a more precise determination of the sensitive mixing zones than the first step based upon the threshold value. It yields a usage factor or similarly an allowable time of operation for a given mixing zone. The so-called $\Delta T=f(t)$ curves relate the temperature difference upstream the mixing zone and the corresponding allowable time before initiating fatigue cracks.

The methodology is based upon a simplified description of the thermal-hydraulic load and the rules specified in the RCC-M guideline [2]. It is now presented in detail.

Thermal-Mechanical Calculations

The main thermal hypotheses are (refer to Fig. 1 for notations) :

- the pipe thickness e is small enough compared to its diameter (inner radius R_{int}) to neglect the pipe curvature,
- the local fluid temperature near the pipe wall is assumed to have a sinusoidal shape with peak-to-peak range set to 80% of ΔT and circular frequency ω, where $\Delta T=T_H-T_C$ is the temperature difference between the hot and cold branches upstream the mixing zone,
- the constant heat transfer coefficient H between the flow and the pipe inner wall is defined for different major classes of piping systems, mainly depending on their size, operating temperature and flow rate ;
- the wall temperature field is solution to the 1D unsteady heat conduction equation for a semi-infinite wall.

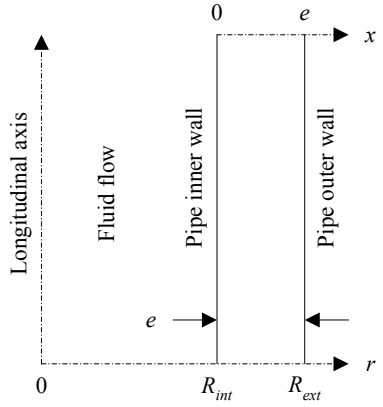

Fig. 1 – Definition of the main geometrical variables

Under these hypotheses, the thermal-mechanical response of the structure can be readily determined from analytical frequency functions defined below. The dimensionless Biot's and Fourier's numbers are introduced, where λ and d are the thermal conductivity and diffusivity of the material, respectively :

$$B=\frac{He}{\lambda},\ F=\sqrt{\frac{e^2\omega}{2d}},\ \bar{x}=\frac{x}{e} \tag{1}$$

For the boundary conditions considered here, the mean temperature inside the wall is equal to that of the fluid. The frequency response functions relating fluid and solid temperature fluctuations can be analytically derived :

$$H_T\left(\bar{x},\omega\right)=z_1\ e^{-(1+j)F\bar{x}}\ \text{ with }\ z_1=\frac{B}{B+(1+j)F} \tag{2}$$

The unsteady temperature profile through the pipe wall can be written as follows :

$$T\left(\bar{x},t\right)=T_{lin}\left(\bar{x},t\right)+\tilde{T}\left(\bar{x},t\right)\ \text{ with }\ T_{lin}\left(\bar{x},t\right)=\Delta T_1(t)\left(\bar{x}-\frac{1}{2}\right)+T_m(t) \tag{3}$$

where $\Delta T_1(t)$ is the unsteady slope of the temperature profile linear part $T_{lin}\left(\bar{x},t\right)$ and $T_m(t)$ its average value throughout the pipe wall, accounting for the pipe curvature. Least-square minimization between $T\left(\bar{x},t\right)$ and $T_{lin}\left(\bar{x},t\right)$ yields :

$$\Delta T_1(t)=12\int_0^1 T\left(\bar{x},t\right)\left(\bar{x}-\frac{1}{2}\right)d\bar{x} \tag{4}$$

The corresponding frequency response functions (H_m for T_m and H_1 for ΔT_1) are given by :

$$H_m(\omega)=\frac{z_1}{2\frac{R_{ext}}{e}-1}\frac{1}{F^2}\left[\left(1-e^{-(1+j)F}\right)\left((1-j)F\frac{R_{ext}}{e}-j\right)-F(1-j)\right],\ H_1(\omega)=-\frac{3z_1}{F^2}\left[\left(F-j\left(F+2\right)\right)\left(e^{-(1+j)F}+1\right)+4j\right] \tag{5}$$

Temperature frequency response functions at the pipe inner wall are exhibited on Fig. 2, illustrating the decay of the thermal response with increasing frequency. The role of the heat transfer coefficient is displayed. The wall thickness does not play a major role in the thermal model as far as the inner wall temperature is concerned.

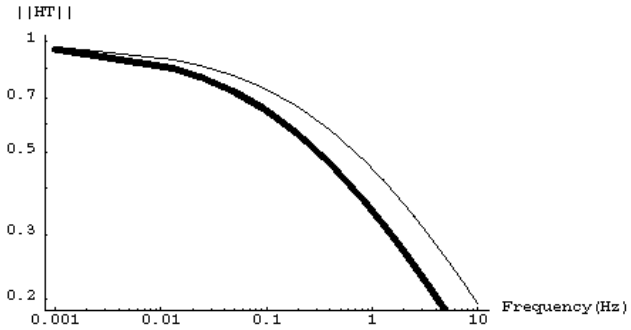

Fig. 2 – Inner wall temperature frequency response function modulus $||H_T||$ for two cases (304L at 150°C)
Thick : e=9.3 mm, H=15000 W.m^{-2}.°C^{-1}, Fine : e=9.3 mm, H=10000 W.m^{-2}.°C^{-1}, R_{int}=127.02 mm

Under the hypothesis of a free end thin pipe evenly submitted to a uniform temperature field, the stress tensor writes, all other terms being equal to zero :

$$\sigma_{zz}(x,t)=\sigma_{\theta\theta}(x,t)=\sigma(x,t)=\frac{E\alpha}{1-\nu}\left(T_m(t)-T(x,t)\right) \tag{6}$$

E is the Young's modulus of the material, ν its Poisson's coefficient and α its expansion coefficient. The peak and linear stresses are defined respectively as follows :

$$S_P(t)=\sigma(x=0,t),\ S_n(t)=\frac{E\alpha}{1-\nu}\frac{\Delta T_1(t)}{2} \tag{7}$$

The corresponding frequency response functions can be easily deduced from those of the temperature fields given in Eq. (5). The shape of the frequency response functions of peak stress can be seen on Fig. 3. Unlike the temperature (see Fig. 2), the stress frequency response exhibits a maximum value at an intermediate frequency which varies with the key parameters (heat transfer coefficient, thickness). The thermal-mechanical response of the pipe to a sinusoidal fluid load also has a sinusoidal shape, with magnitude and phase angle related to those of the fluid by the frequency response functions.

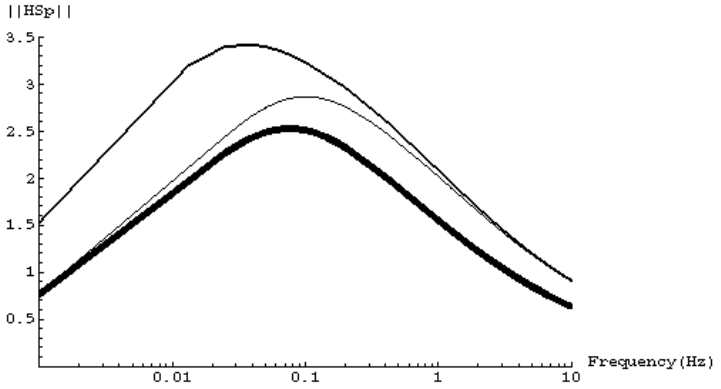

Fig. 3 – Comparison of peak stress frequency response function modulus $||H_{Sp}||$ for three cases (304L at 150°C)
Thick : e=9.3 mm, H=10000 W.m^{-2}.°C^{-1}, Medium : e=20 mm, H=15000 W.m^{-2}.°C^{-1}
Fine : e=9.3 mm, H=15000 W.m^{-2}.°C^{-1}, R_{int}=127.02 mm

Fatigue Analysis (Crack Initiation)

The definition of a method for crack initiation analysis requires to consistently set the description of the fluid thermal load, choose a thermal-mechanical model and select fatigue criteria.

In our case, the fatigue analysis is based upon the rules specified in RCC-M guideline [2]. The alternating stress S_{alt} needed as input in the S-N design curves for damage calculation is deduced from the sinusoidal stress field obtained beforehand :

$$S_{alt} = K_{eth} \frac{\Delta S_p^{'}}{2} \frac{E_{SN}}{E} \tag{8}$$

where E_{SN} is the Young's modulus of the S-N fatigue curve.

$\Delta S_p^{'}$ is the peak-to-peak range of $S_p^{'}$ which accounts for the existence of rough (K_3=1,7) or leveled (K_3=1,1) welds (K_3=1 otherwise) :

$$S_p^{'} = S_p + (K_3 - 1) S_n \tag{9}$$

K_{eth} is the elastic-plastic strain correction factor defined as follows for stainless steel (K_{eth}=1 otherwise) :

$$K_{eth} = max\left(1\,;\,1{,}86\left(1 - \frac{1}{1{,}66 + \frac{\Delta S_n}{S_m}}\right)\right) \tag{10}$$

where S_m denotes the allowable stress of the material and ΔS_n the peak-to-peak range of S_n.

The damage is inferred from the proper RCC-M S-N design curve. >From the alternating stress at a given temperature difference upstream the mixing zone, the S-N curve yields the maximum allowable number of cycles N_{all} which can be easily converted into an allowable operating time t_{all}. As the result depends on the frequency of the load, the minimum value of t_{all} is estimated with respect to the frequency. Damages are then combined for different conditions (ΔT) in a linear way.

The determination of the threshold values used in the first step of the procedure to select the sensitive mixing zones is consistent with the lowest ΔT value leading to a non zero value of damage according to the calculation described above. In fact, it corresponds to the endurance limit of the material fatigue curve.

Concerning the second step of the screening criteria of the sensitive mixing zone, the overall process of this so-called $\Delta T=f(t)$ method is illustrated on Fig. 4. It has been successfully compared to in-situ damages observed on a large database of RHRS mixing zones whose operating conditions (ΔT, t) had been previously determined. The industrial method always estimated conservative damages, as depicted on Fig. 5.

Figure 6 gives several examples of $\Delta T=f(t)$ curves and their sensitivity to the key parameters (ΔT, H, e).

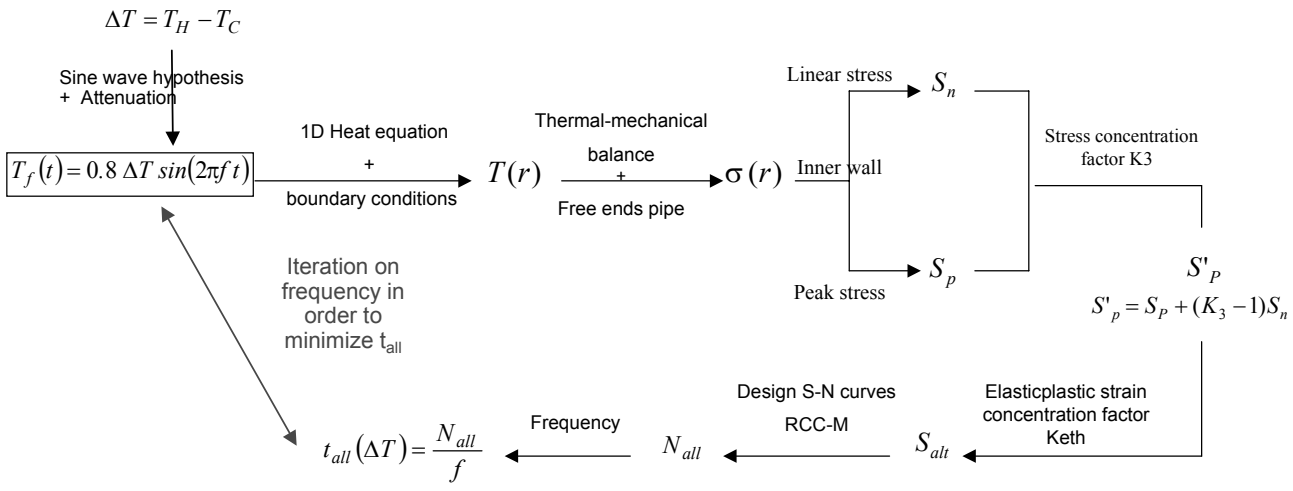

Fig. 4 – Procedure diagram for crack initiation method

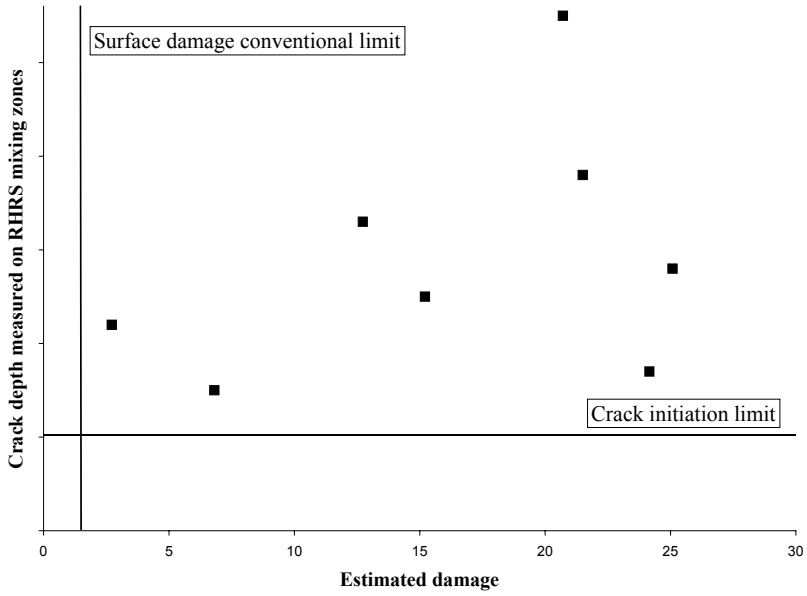

Fig. 5 – Crack initiation method : comparison between estimated damages and crack depths

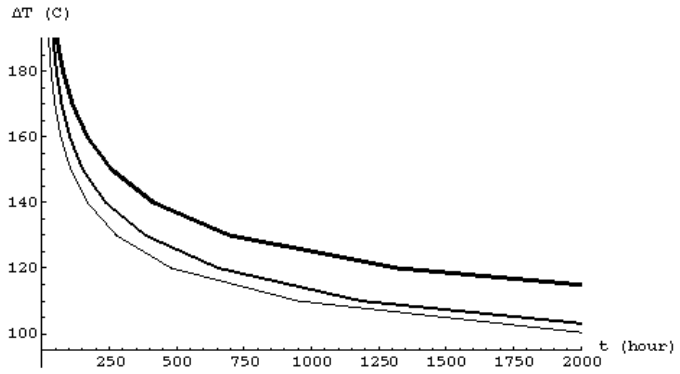

Fig. 6 – $\Delta T=f(t)$ curves for rough welds (304L at 150°C) : Thick : e=9.3 mm, H=10000 W.m^{-2}.°C^{-1} Medium : e=20 mm, H=15000 W.m^{-2}.°C^{-1}, Fine : e=9.3 mm, H=15000 W.m^{-2}.°C^{-1}, R_{int}=127.02 mm

DETAILED ANALYSIS OF MIXING ZONES SENSITIVE TO THERMAL FATIGUE

The previous procedure allowed us to determine the sensitivity of mixing zones with given operating conditions and material characteristics as far as the onset of surface cracks is concerned.

A refined analysis of defect initiation which would alleviate the severity of the present method is not yet available for engineering industrial applications. Research and Development work is detailed in a subsequent section.

It is nevertheless of high importance to evaluate the risk of a supposedly initiated crack to reach the size of a critical defect which would lead to the rapid failure of the pipe. For this safety analysis, fatigue propagation of an incipient crack then has to be estimated. It also helps to assess the in–service inspection program. Again, conservative assumptions and hypotheses are used to infer the growth of a crack of initial depth a_0 and eccentricity c_0/a_0.

Thermal-Mechanical Hypotheses

As presented earlier, the structure is assumed to have a linear one-dimensional thermal behavior. At this point, the finite thickness of the pipe wall has to be accounted for, as we are dealing with crack of depth possibly reaching a significant amount of the overall thickness. We wish the reader will take it for granted that a fully analytical solution of the equations can also be derived in this case, in a way quite similar to the case of a semi-infinite wall, though somewhat more painstakingly. The frequency response function between fluid and wall temperatures writes :

$$H_T(\bar{x},\omega) = z_2\ S_2(\bar{x}) \text{ with } z_2 = \frac{B}{(1+j)F\ sh[(1+j)F] + B\ ch[(1+j)F]} \text{ and } S_2(\bar{x}) = z_2\ ch[(1+j)F(1-\bar{x})] \qquad (11)$$

The integration of the above expression yields the following frequency response function for the mean temperature through the wall, neglecting the pipe curvature :

$$H_m(\omega) = z_2 \; S_1 \text{ with } S_1 = \frac{z_2}{2F}(1-j)\, sh[(1+j)F] \tag{12}$$

The stress field is given by Eq. (6). Its frequency response function can be deduced from Eq. (11) and Eq. (12).

Thermal-Mechanical Response Calculation

Unlike the crack initiation method, the propagation analysis relies on a realistic random time-history of the fluid temperature. This thermal-hydraulic load is generally recorded on a reduced scale mock-up of the mixing zone.

The structure being modeled as an ideal linear system, its thermal and mechanical response can be characterized by its unit-impulse response function *h(t)*. The output *s(t)* (temperature, strain, stress) of such a system is related to the input *e(t)* (fluid temperature load) as follows :

$$s(t) = h \otimes e(t) = \int_0^{\infty} h(\tau)\, e(t-\tau)\, d\tau \tag{13}$$

For a random stationary process, it is equivalent to consider the frequency response function of the system, corresponding to the Fourier Transform of the unit-impulse response function. The convolution integral in Eq. (13) can then be determined using the Fast Fourier Transform algorithm (*FFT*) :

$$s(t) = Re\left[FFT^{-1}\left(H(\omega) \times FFT(e(t))\right)\right] \tag{14}$$

where Re denotes the real part of a complex variable.

Figure 7 features the stress and temperature Power Spectral Density (PSD) functions measured at the outer wall of a mixing zone. An excellent correlation is obtained between both PSD functions with the above frequency response functions, giving us reasonable confidence in the thermal-mechanical model.

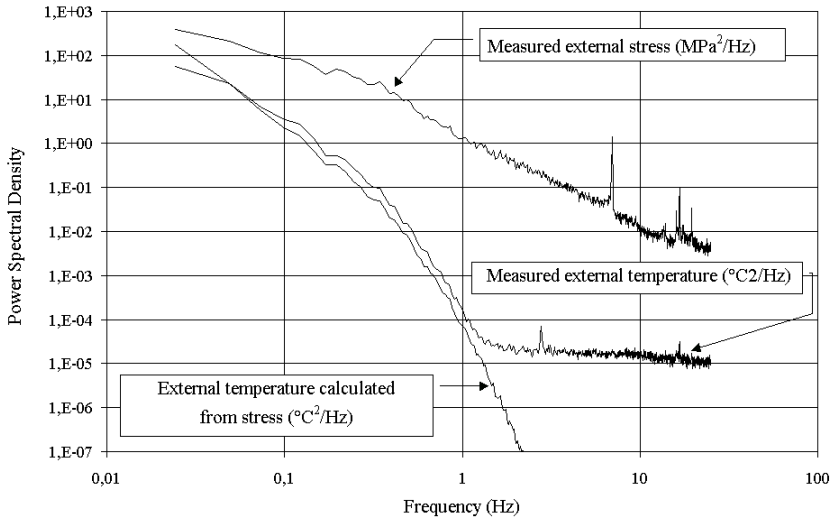

Figure 7 – Comparison of temperature PSD measured at the outer wall of a mixing zone and calculated from the corresponding measured stress (304L stainless steel at 150°C, *e*=7.11 mm, *H*=15000 $W.m^{-2}.°C^{-1}$)

Crack Growth Calculation

The propagation analysis methodology is based upon the RSE-M codified approach [3]. It first requires to determine the stress intensity factor K_I whose calculation from the stress field time-history is now briefly presented, according to the influence coefficient method. The stress intensity factor writes :

$$K_I(t) = \sqrt{\pi\, a} \sum_{k=0}^{3} \left(\frac{a}{L}\right)^k i_k \sigma_k(t) \tag{15}$$

where the influence functions i_k, depending on the relative crack depth *a/e*, the crack eccentricity *a/c* and the pipe curvature R_{int}/e, are determined by a barycentric interpolation from the RSE-M tabulated values and where the time-dependent coefficients $\sigma_k(t)$ arise from a polynomial fit of the stress profile in the pipe wall. The coefficients $\sigma_k(t)$ are determined with the minimization of the following variable over a length *L* in the pipe thickness :

$$\int_1^{1-\frac{L}{e}} \left[Re\left(\sigma(\bar{x},t)\right) - P(\bar{x},t)\right]^2 d\bar{x} \quad \text{where} \quad P(\bar{x},t) = \sum_{k=0}^{3} \sigma_k(t) \left(\frac{e}{L}\right)^k (1-\bar{x})^k \text{ , with } 1-\frac{L}{e} \le \bar{x} \le 1 \tag{16}$$

The tedious mathematical derivation of the above expression leads to a fully analytical form of the polynomial stress coefficient frequency response function with respect to the temperature fluid load. The main relations are :

$$\forall\, k = 1 \text{ to } 3, \qquad \delta_k = p\delta_k\left(1-\frac{L}{e}\right) - p\delta_k(1), \quad HY_{\Lambda_k}(\omega, L) = -\frac{e}{L}\frac{2E\alpha}{1-\nu} z\left[-\frac{L}{e}\frac{1}{k+1}S_1 - \left(\frac{e}{L}\right)^k \delta_k\right] \tag{17}$$

$$p\delta_0(\bar{x}) = \frac{1}{2F}(1-j)sh\left[(1+j)F\bar{x}\right], \; p\delta_1(\bar{x}) = (1-\bar{x})p\delta_0(\bar{x}) - \frac{j}{2F^2}S_2(\bar{x}) \tag{18}$$

$$p\delta_2(\bar{x}) = \left[(1-\bar{x})^2 - \frac{j}{F^2}\right]p\delta_0(\bar{x}) - \frac{j}{F^2}(1-\bar{x})S_2(\bar{x}) \tag{19}$$

$$p\delta_3(\bar{x}) = (1-\bar{x})\left[(1-\bar{x})^2 - \frac{3j}{F^2}\right]p\delta_0(\bar{x}) - \frac{3j}{2F^2}\left[(1-\bar{x})^2 - \frac{j}{F^2}\right]S_2(\bar{x}) \tag{20}$$

$$H\sigma_0(\omega, L) = -70\, HY_{\Lambda_3}(\omega, L) + 120\, HY_{\Lambda_2}(\omega, L) - 60\, HY_{\Lambda_1}(\omega, L) + 8\, HY_{\Lambda_0}(\omega, L) \tag{21}$$

$$H\sigma_1(\omega, L) = 840\, HY_{\Lambda_3}(\omega, L) - 1350\, HY_{\Lambda_2}(\omega, L) + 600\, HY_{\Lambda_1}(\omega, L) - 60\, HY_{\Lambda_0}(\omega, L) \tag{22}$$

$$H\sigma_2(\omega, L) = -2100\, HY_{\Lambda_3}(\omega, L) + 3240\, HY_{\Lambda_2}(\omega, L) - 1350\, HY_{\Lambda_1}(\omega, L) + 120\, HY_{\Lambda_0}(\omega, L) \tag{23}$$

$$H\sigma_3(\omega, L) = 1400\, HY_{\Lambda_3}(\omega, L) - 2100\, HY_{\Lambda_2}(\omega, L) + 840\, HY_{\Lambda_1}(\omega, L) - 70\, HY_{\Lambda_0}(\omega, L) \tag{24}$$

The frequency response function of the stress intensity factor K_I is easily deduced from Eq. (15) and Eq. (17) to Eq. (24). For a mean stress load σ_m, the stress intensity factor is given by :

$$K_m(\sigma_m, a, c) = \sqrt{\pi\, a}\; i_0\left(\frac{R_{int}}{e}, \frac{a}{e}, \frac{a}{c}\right)\sigma_m \tag{25}$$

As presented earlier, the stress intensity factor time-history is easily deduced from the fluid load, assuming a stationary process. Its average value is adjusted with the mean stress, according to Eq. (25). The Rain-Flow algorithm [4] then provides us with the stress intensity factor cycles (ΔK, K_{min}, K_{max}) over the time-history considered.

For each cycle, a plasticity correction yields the effective stress intensity factor ΔK_{eff} as follows :

$$\Delta K_{eff} = \Delta K_{cp}\; f(R) = \alpha_{cp}\Delta K\sqrt{1+\frac{r_y}{a}}\; f(R), \; \Delta K = K_{max} - K_{min}, \; R = \frac{K_{min}}{K_{max}} \tag{26}$$

$$f(R) = \frac{1}{1-\frac{R}{2}} \quad if\; K_{min} \geq 0, \; f(R) = Max\left[\frac{1}{3}; \frac{1}{1-\frac{R}{2}}\right] \quad if\; K_{min} < 0 < K_{max}, \; f(R) = \frac{1}{3} \quad if\; K_{min} < K_{max} < 0 \tag{27}$$

$$r_y = \frac{1}{6\pi}\left(\frac{\Delta K}{2\sigma_y}\right)^2, \; \alpha_{cp} = 1 \quad if\; r_y \leq 0{,}05\,(e-a), \alpha_{cp} = 1 + 0{,}15\left(\frac{r_y - 0{,}05\,(e-a)}{0{,}035\,(e-a)}\right)^2 \quad if \begin{cases} 0{,}05\,(e-a) \leq r_y \\ and\; r_y \leq 0{,}085\,(e-a) \end{cases} \tag{28}$$

A basic Paris's law is used to infer the crack growth :

$$\frac{da}{dN} = k_0\left(\Delta K_{eff}\right)^{N_0} \tag{29}$$

Provided Δa remains small enough over the time step Δt, we obtain :

$$\Delta a(\Delta t, a) = k_0 \sum_{cycles}\left(\Delta K_{eff}(\omega, a)\right)^{N_0} \tag{30}$$

The main shortcoming of the influence coefficient method comes from the polynomial fit of the stress variations in the wall. The smoothing may indeed deviate from the original profile for high frequencies or when the crack length becomes too large.

R&D PROGRAMS

A R&D program is currently under way at EDF [5] to improve these methodologies. Some studies are done together with FRAMATOME ANP and CEA or in a European framework [6, 7].

Part of the program is dedicated to a more realistic description of the fluid thermal load, including the evaluation of fluid-structure transfer. To this end, a large experimental database is used, from intrusive mock-up tests simulating various kinds of mixing zones to in-situ outer wall temperature and strain measurements. The issue of relevant scaling laws needed to apply experimentally determined fluid loads on actual industrial configurations is particularly examined. The capability of advanced computational techniques to assess the turbulent fluctuations in mixing zones is also evaluated [8]. In the prospective search for an advanced crack initiation method, it is needless to try to improve the thermal load description without evaluating the other parameters or hypotheses of the method. Thus, the R&D program also includes a large series of tests for the determination of 304L and 316L material properties (fatigue curves, cyclic stress-strain curves), with different parametric studies on temperature, mean stress, surface finish and PWR environment effects [9]. It particularly focuses on the high number of cycles range of the fatigue curve (10^5 to 10^7). Complementary thermal fatigue analytical tests are carried out at both CEA and EDF. Besides, thermal-mechanical and fatigue modeling issues are also addressed. They are meant to assess the computation of stresses in complex structures under complex thermal loads and to evaluate alternative fatigue evaluation procedures under multi-axial random loads.

A final demonstration test is currently under way at CEA. A 6 inch. mixing tee is subjected to upstream flows with a high temperature difference (around 160°C) over a long period of time (several hundreds of hours, typically). Crack initiation is monitored at regular time intervals using external Ultrasonic Testing. The thermal loads will be measured in the same conditions. This test will provide us with useful data to evaluate existing and future methodologies for fatigue initiation in mixing zones.

CONCLUSION

The different steps of crack initiation and propagation analyses for pipes submitted to mixing zone thermal fatigue have been described. To the authors' knowledge, it is the first time that a fully analytical solution of the 1D linear elastic model is exhibited, from the temperature and strain fields through the wall to the stress intensity factor.

Both methodologies are currently used at EDF for industrial purposes concerning mixing zones. Besides, they are known to be conservative. Using the proposed step by step procedure, the number of detailed analysis is limited to three to five tees or nozzles by plant, three of them are class 1 nozzles (charging line, surge line, safety injection line) and one of class 2 (auxiliary feedwater nozzle).

ACKNOWLEDGMENTS

The authors are grateful to Mr Lebouleur, who initiated this work during its graduate training period in 2000, and to Mr Grousset who performed most of the derivations and calculations. They also express their thanks to all contributors from EDF R&D and engineering divisions as well as from the plant operation headquarters, who supported this work and provided valuable applications.

REFERENCES

1 Faidy C., High Cycle Thermal Fatigue : Lessons Learned From Civaux Event. 2nd International Conference on Fatigue of Reactor Components, Snowbird, Utah, July 29-31, 2002.
2 RCC-M, Design and construction rules for mechanical components of PWR nuclear islands. AFCEN (2000).
3 RSE-M, Surveillance and in-service inspection rules for mechanical components of PWR nuclear islands. AFCEN (1997 edition, addenda 1998 and 2000).
4 Technical standard AFNOR A03-406 Produits métalliques – Fatigue sous sollicitations d'amplitude variable – Méthode Rain-Flow de comptage des cycles. AFNOR.
5 Stephan J.M. et al., Evaluation of the Risk of Damages in Mixing Zones : EDF R&D program. 2nd International Conference on Fatigue of Reactor Components, Snowbird, Utah, July 29-31, 2002.
6 Metzner K. et al., Status Report : European THERFAT Project – Thermal Fatigue Evaluation of Piping System Tee-connections. 2nd International Conference on Fatigue of Reactor Components, Snowbird, Utah, July 29-31, 2002.
7 Chapuliot S. et al., OECD Benchmark Proposal on Thermal Fatigue Problem. 2nd International Conference on Fatigue of Reactor Components, Snowbird, Utah, July 29-31, 2002.
8 Peniguel C. et al., Presentation of a numerical 3D approach to tackle thermal striping in a PWR nuclear T-junction. Cleveland, Ohio, ASME PVP, July 20-24, 2003.
9 Amzallag C., High Cycle Fatigue Behavior of Austenitic Stainless Steel. 2nd International Conference on Fatigue of Reactor Components, Snowbird, Utah, July 29-31, 2002.